SPIE Smart Structures, Feb. 1996.

A CMOS-compatible, surface-micromachined pressure sensor for aqueous ultrasonic application

W.P. Eaton* and J.H. Smith
Integrated Micromechanics, Microsensors, & CMOS Technologies Department
Sandia National Laboratories
Albuquerque, NM 87185-1080

Keywords: surface micromachining, MEMS, CMOS, pressure sensor, pressure transducer, vacuum encapsulated

ABSTRACT

A surface micromachined pressure sensor array is under development at the Integrated Micromechanics, Microsensors, and CMOS Technologies organization at Sandia National Laboratories. This array is designed to sense absolute pressures from ambient pressure to 650 psia with frequency responses from DC to 2 MHz. The sensor is based upon a sealed, deformable, circular LPCVD silicon nitride diaphragm. Absolute pressure is determined from diaphragm deflection, which is sensed with low-stress, micromechanical, LPCVD polysilicon piezoresistors. All materials and processes used for sensor fabrication are CMOS compatible, and are part of Sandia's ongoing effort of CMOS integration with Micro-ElectroMechanical Systems (MEMS). Test results of individual sensors are presented along with process issues involving the release etch and metal step coverage.

2. INTRODUCTION

Recently, there has been a trend towards developing smart sensors as a part of a larger effort to improve instrumentation. In this paper we present a piezoresistive, surface-micromachined pressure sensor. The sensor is based upon a sealed silicon nitride diaphragm and senses absolute pressure. All materials and processes used for sensor fabrication are CMOS compatible, and are part of the ongoing effort of CMOS integration with MEMS at Sandia National Laboratories' Microelectronics Development Laboratory. The pressure sensor will be used as a basic building block to complement other sensor technologies[1]. Also, as part of Sandia's defense related activities, the sensor may be used for treaty verification/non-proliferation or weapons' state-of-health monitoring. Furthermore, the sensor may find applications in the automotive, aerospace, biomedical, and electronics industries.

In the automotive industry, which has been a driving force for high-volume sensor technology, sensors are needed for air bag and anti-lock brake deployment, cabin temperature regulation, engine combustion optimization, and suspension control. In the aerospace industry, smart sensors are desired to fully characterize wing conditions. Such characterizations can be used to improve stability in fly-by-wire control systems. In the arena of biomedical research, researchers are trying to measure conditions inside the human body, a capability that is becoming increasingly feasible as sensors shrink in size. Furthermore, in virtually any manufacturing setting, it is desirable to closely monitor processing conditions for use in statistical process control.

Micromachining technology is well suited for developing smart sensors, for the following reasons:

- Accuracy – many microsensors have equaled or exceeded the accuracy of their larger counterparts[2]
- CMOS Compatibility– microsensors can be built side-by-side with integrated circuits
  - Low power consumption
  - Built in signal conditioning & compensation
  - Digital output
  - Batch fabrication
- Small Form Factor– packaged microsensors are small and lightweight.

* Under contract from the Center for High Technology Materials, The University of New Mexico, Albuquerque, NM 87131.

This work was performed and supported at Sandia National Laboratories by the U.S. Department of Energy under contract DE-AC04-94AL85000

3. GOALS

The principal goal of the project was to develop a robust, wide-range pressure sensor technology. Specific goals include:

- CMOS compatibility– all fabrication process steps compatible with CMOS technology
- Pressure range and response time
  - 1 to 10 atmospheres
  - DC to 2 MHz
- Operating environments
  - gaseous (including air)
  - aqueous
  - severe (e.g. corrosive).

4. BASIC OPERATION

A schematic representation of the pressure sensor is shown in Figure 1. It consists of a circular silicon nitride diaphragm. The diaphragm forms the top of a sealed vacuum cavity, which provides a reference pressure. Polysilicon strain gauges are mounted on top of the diaphragm. As the membrane deflects due to an applied pressure, the edges of the diaphragm are placed in radial tensile strain, while the center is placed in circumferential compressive strain. This behavior causes resistance changes in the radial and circumferential strain gauges that are equal, but opposite in sign. To first order, the resistance changes are directly proportional to the applied pressure.

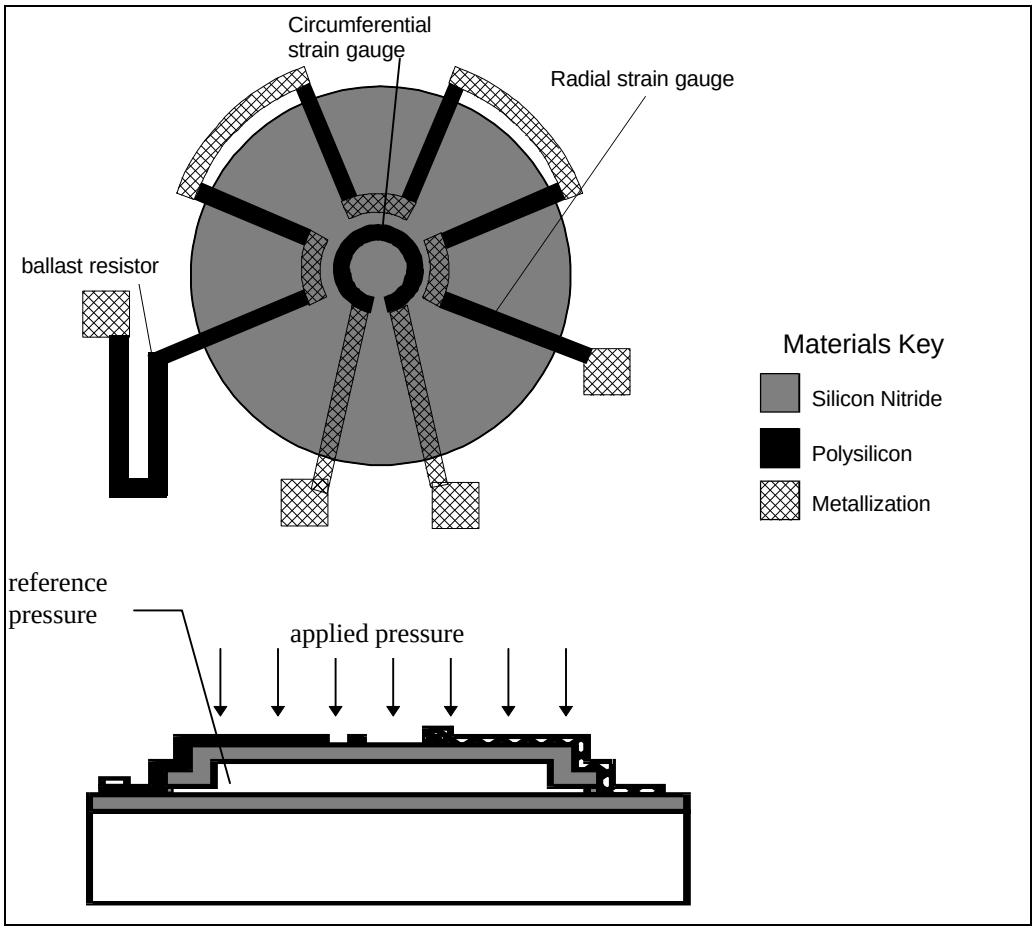

Figure 1. Schematic of pressure sensor.

5. DESIGN

5.1 Materials

The goals stated previously impacted the choice of materials available for fabrication of the pressure sensor. Some of the available materials that were CMOS compatible were: LPCVD silicon nitride, CVD doped and undoped glasses (i.e. TEOS, PSG, BPSG), LPCVD polysilicon, and sputtered aluminum metallization. Polysilicon piezoresistive strain sensors were used to insure CMOS compatibility. Although piezoelectric materials can also be used in pressure sensors, these materials such as zinc oxide or lead zirconium titanate pose contamination issues in a CMOS line. Additionally, operation in ionic, aqueous environments precludes the use of capacitive transduction.

The diaphragms were fabricated from low-stress silicon nitride, which is non-stoichiometric, silicon-rich, and slightly tensile. Silicon nitride was chosen as the diaphragm material because it is both electrically insulating, chemically resistant and mechanically tough.

5.2 Diaphragm Geometry

The required pressure ranges and response times affect the allowed geometry of the pressure sensor. The theoretical frequency response of a diaphragm has a pole at the resonant frequency. Above the resonant frequency, the response of the

diaphragm to pressure waves drops and phase fluctuations are introduced. In general, it is desirable to design diaphragms so that their fundamental resonant frequency is significantly greater than the frequency range of interest.

In the simplest case where no built-in diaphragm stresses are present, the resonant frequency for an edge-clamped circular plate is given by Morse[3] as

$$f_0 = \frac{\pi h}{4a^2}\beta^2\sqrt{\frac{E}{3\rho(1-\nu^2)}} \propto \frac{h}{a^2} \qquad (1).$$

Where f_0 is the resonant frequency, a, h, E, ρ, and ν are the radius, thickness, Young's modulus, mass density, and Poisson's ratio for the diaphragm, and $\beta = 1.017$ for the fundamental frequency. This formula for resonant frequency is contrasted with the pressure sensitivity (amount of output signal per unit applied pressure), which is given by Burns[4] as proportional to a^2/h^2. Hence, a design trade off must be made between sensitivity and frequency response. For good frequency response, a thick diaphragm with small diameter is desirable. The converse is true for good sensitivity. A thorough discussion of these design considerations is provided by Burns.[4]

5.3 Signal detection

Signal detection is accomplished by connecting the piezoresistive strain gauges in a Wheatstone bridge configuration. This approach has several advantages: 1) first order compensation of common mode signals such as temperature 2) voltage output, which is easily measured, and 3) relative immunity to changes in supply voltage. A current loop detection scheme also has similar advantages[5,6], but has more complicated instrumentation requirements.

6. SENSOR ARRAYS

Seven sizes of diaphragms were designed. All diaphragms deflect a maximum of 2μm, which is determined by the thickness of the layers of sacrificial oxide (see fabrication sequence). Resonant frequencies, normalized sensitivities, and maximum applied pressure before full deflection are calculated from membrane dimensions and are shown in Table 1. By using an array of diaphragm sizes, the trade off between frequency response and sensitivity is ameliorated. Both high sensitivity and good frequency response can be achieved in one small package. With the further refinement of on-chip circuitry, the signals could be processed so that the output is self-selecting to the most sensitive transducers, self-calibrating, and self- temperature compensating. Overpressure bursting of larger membranes while operating in the pressure regime of the smaller membranes is not expected to be an issue, since the diaphragm travel will be stopped by the underlying substrate. Overpressure behavior of similar surface micromachined pressure sensors has been reported by other researchers.[7]

h [μm]	a [μm]	f_0[MHz]	P_{max} [psia]	Normalized Sensitivity
0.8	25	7.0	650	1
0.8	50	1.8	41	4
0.8	75	0.78	8.0	9
0.8	100	0.44	2.5	16
0.8	125	0.28	1.0	25
0.8	250	0.070	0.06	100
0.8	500	0.018	0.004	400

Table 1. Theoretical diaphragm characteristics with varied diaphragm radius.
Materials constants for Si_3N_4: E=300 [GPa], ρ= 2330 [Kg/m^3], ν= .25

7. FABRICATION

7.1 Fabrication Sequence

The fabrication sequence of the sensor is shown schematically in Figure 2 and in optical and electron micrographs in Figure 3. The first step is to deposit a 0.8μm thick base layer of low stress silicon nitride film (Figure 2a). This acts as a insulating base layer for resistor and metal lines, and as a non-stick layer so that a fully deflected membrane is less likely to adhere to the substrate. Subsequently, a thick 2μm film of CVD SiO_2 (oxide) is deposited and patterned (Figure 2b and Figure 3a). Then, a thinner 0.1μm layer of CVD SiO_2 is deposited and patterned (Figure 2c). The combined thickness of the thin and thick oxides determine the maximum allowable diaphragm deflection.

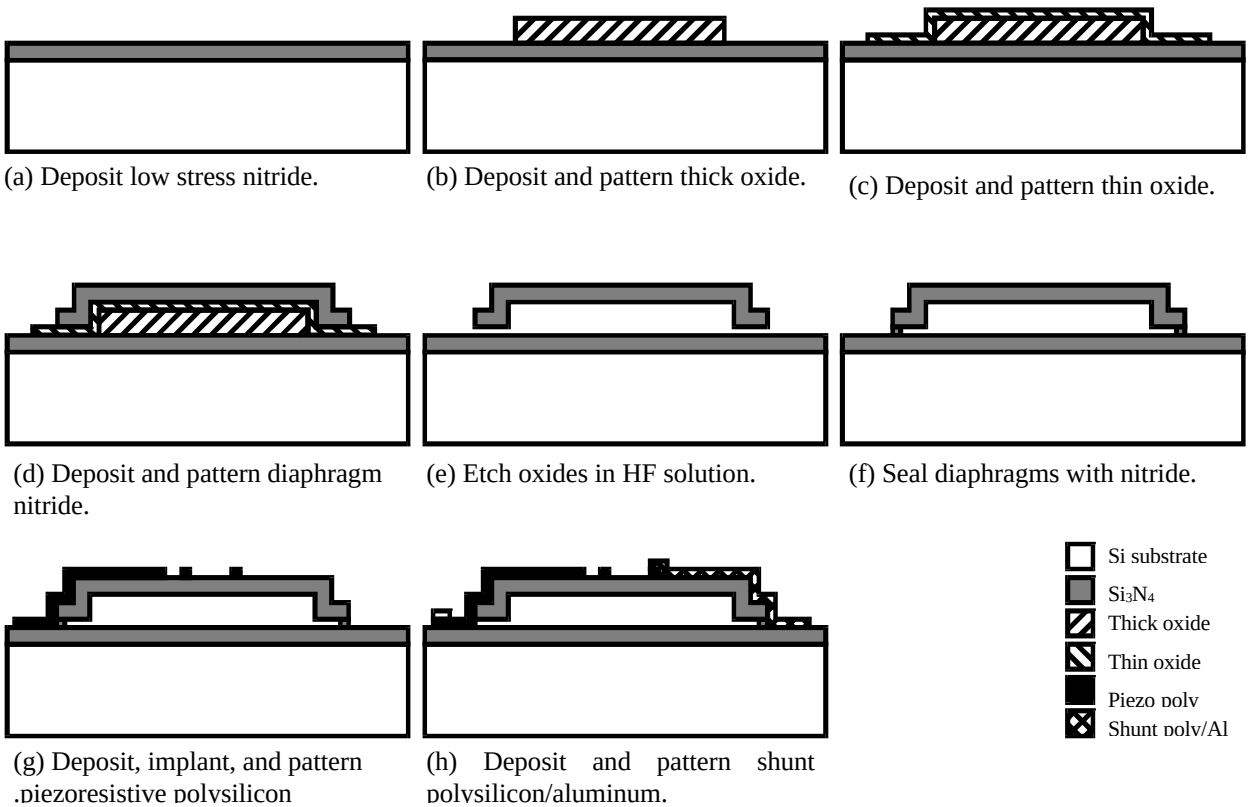

Figure 2. Schematic fabrication sequence of microsensors.

Following the oxide deposition steps, another 0.8μm film of low-stress silicon nitride is deposited and patterned (Figure 2d). This layer of nitride is the diaphragm material, and is anchored to the base layer of nitride through cuts in the sacrificial oxide layers. Figure 3(b) shows a nitride membrane after this deposition but before patterning. After patterning, thin oxide stubs are exposed. These thin oxide stubs allow enchant to reach the oxide layers underneath the diaphragm during the release etch. The devices are placed in an HF-based, release etch solution. This solution removes the oxide layers beneath the diaphragm, thus freeing the diaphragm. Figure 3(c) shows a partially-released 100μm-diameter diaphragm. The white material in the center is unetched oxide beneath the nitride diaphragm. A fully-released 50μm diaphragm is shown in Figure 3(d), with the inset showing a close-up of one of the etch ports. The etch port was enlarged during the oxide etch by the HF. This removal of the nitride by HF will be discussed in Section 7.2. After the oxide has been etched away in the HF solution, the wafers are dilution rinsed with deionized water, removed from the water, and allowed to air dry.

Following the drying process, the diaphragms are sealed by another low-stress nitride deposition of ~0.1μm, which plugs the etch ports. If the etch ports are significantly enlarged during the HF etch, the sealing layer thickness must be increased. Ideally, without the attack of the nitride during the release etch, the minimum thickness of the sealing layer would be half the thickness of the thin oxide. Deposition conditions during the sealing step are 850°C and 250 mTorr, so

the residual pressure at room temperature (assuming ideal gases) should be ≈67 mTorr. Some researchers have reported residual pressures of 200-300 mTorr[8] for nitride sealing, and in general, the actual pressure, though stable for any given diaphragm, is variable and non-repeatable across a substrate and from substrate to substrate. However, since residual pressures are under 1 Torr, the pressure variations are insignificant relative to the sensitivity of the sensors for pressure measurements at or above ambient pressure. Other sealing techniques can be used, such as polysilicon deposition[8] or reactive oxide sealing.[4]

fix fab seq.Once the diaphragms have been sealed, special rinsing and drying techniques are no longer needed. Processing continues with the deposition and ion implantation of the polysilicon piezoresistors. An implant of phosphorus at 80 keV with a dose of $3 \cdot 10^{14}/cm^2$ was chosen to maximize the gauge factor of the polysilicon.[9] After implant, the polysilicon is patterned. Then a layer of heavily doped shunt polysilicon is deposited and patterned. The purpose of this shunt layer is to mitigate problems associated with the step coverage of aluminum over the diaphragm edges and will be discussed in Section 7.2. Finally, aluminum metallization is deposited and patterned, and the devices are ready to be tested. For corrosion resistance, an additional silicon nitride layer will be deposited and patterned as a passivation layer.

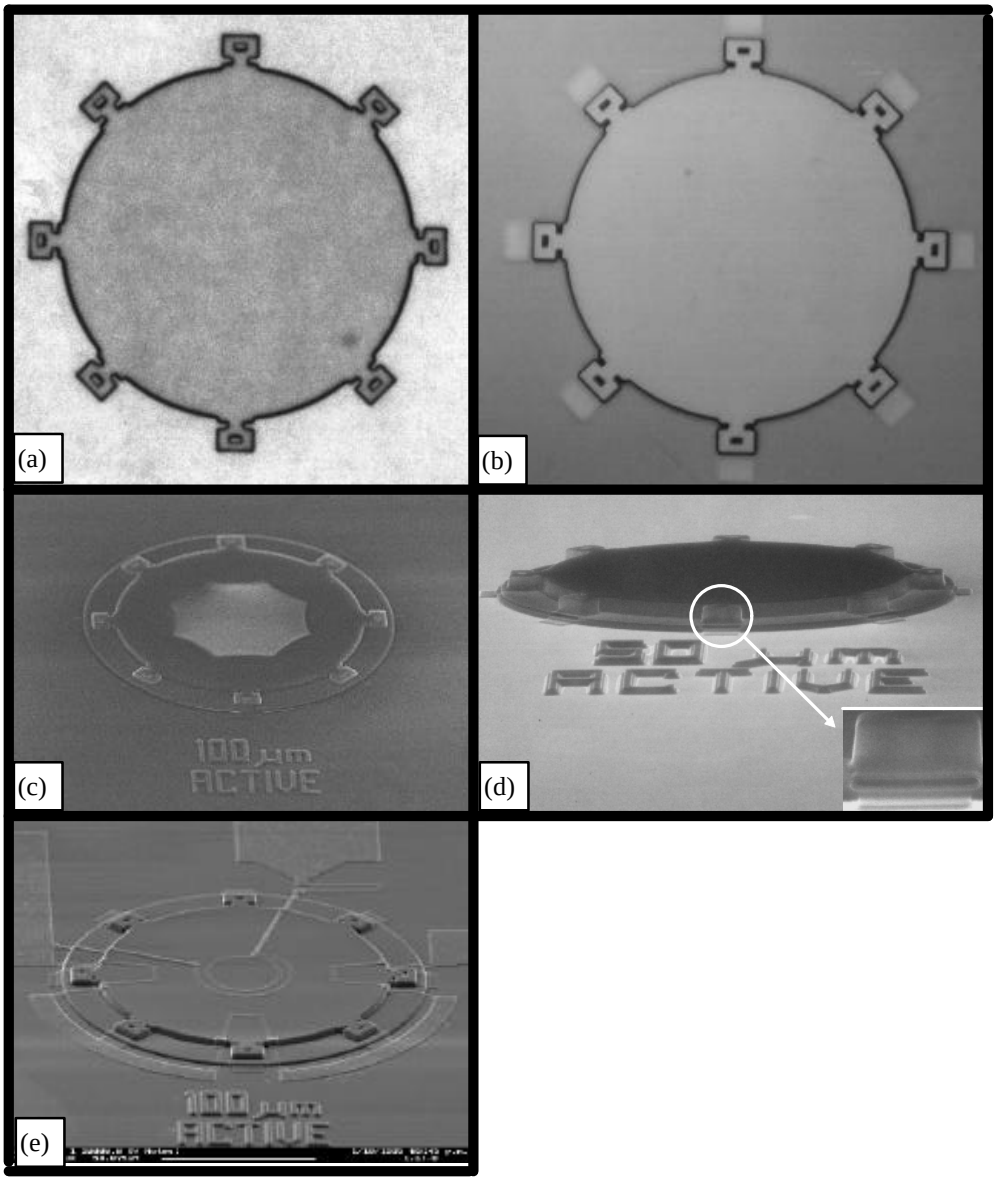

Figure 3. Optical[(a),(b)] and electron[(c)-(e)] micrographs of fabrication sequence. (a) 100µm diameter thick oxide after patterning. (b) 100 µm diameter diaphragm after diaphragm deposition. (c) Partially released 100µm diameter diaphragm. (d) Fully released 50µm diameter diaphragm. (e) Completed 100µm diameter pressure sensor.

7.2 Fabrication Issues

One of the fabrication issues for the pressure sensor was removal of the silicon nitride during the oxide etch. As would be expected from the removal of nitride during the release etch, larger diaphragms could not initially be released without completely removing the diaphragm material. Furthermore, larger sealing layer thicknesses (~ 0.4 µm) were required because the etch ports were significantly enlarged (inset Figure 3(d)).

This process issue was addressed in two ways: 1) by changing the wet etch chemistry and 2) by using faster etching, thin oxides. The wet etch chemistry was changed from a 1:1 HF:H_2O solution to a 1:1 HF:HCl solution. This yielded both faster oxide etch rates and slower nitride etch rates; providing a much greater etch selectivity of the oxide to silicon nitride. These results are summarized in Table 2. Detailed discussion of these etch conditions are given by Chang.[10]

Etchant	Nitride etch rate [µm/hr]	Oxide etch rate [µm/hr]	Selectivity
1:1 HF:H_2O	0.22	20	91
1:1 HF:HCl	0.12	37	310

Table 2. Oxide etch rates for CVD SiO_2 densified at 1050°C for 30 min.

Several different oxides were used for the fast etching thin oxide experiment:

- densified (1050°C, 30 min.) CVD SiO_2 film as a control
- ion implanted (P, $8 \cdot 10^{15}/cm^2$, 50keV), densified CVD SiO_2
- 2% phosphosilicate glass (PSG)
- 5%/5% borophosphosilicate glass (BPSG).

The PSG and BPSG films were capped in-situ with a 100Å film of undoped SiO_2 to reduced moisture absorption. Absorbed moisture can outgas in later processing steps and lead to film blistering. In a thin oxide/thick oxide sandwich with a fast etching thin oxide, the net lateral etch rate will approach the etch rate of the fast etching oxide. Oxide etch rates for these films are shown in Table 3. As expected, the BPSG films etched the fastest. The effects of using doped glasses is presently being investigated.

Thin oxide	Lateral etch rate [µm/hr]
CVD SiO_2	37
implant	50
PSG	68
BPSG	250

Table 3. Fast etching thin oxide etch rates

A second, important, fabrication issue was poor aluminum step coverage over the diaphragm edge. Sputtered aluminum has poor coverage over steps that exceed its film thickness. The aluminum thickness in the sensors was 0.1 µm and there were 2 µm steps over the diaphragm edges. Hence, a step coverage problem was expected. This problem was avoided by depositing a 0.1 µm-thick layer of heavily doped polysilicon, the "shunt layer", before depositing the aluminum. LPCVD polysilicon has conformal step coverage. Both the polysilicon and aluminum layers were patterned with the same mask. The shunt layer carries current wherever there is an open in the aluminum over a diaphragm edge, while the lower resistivity aluminum carries current over planar regions.

8. Results and Discussion

Several device lots were fabricated and tested. The results for two 100µm diameter diaphragms connected in fully active full bridge configuration, along with a circuit schematic are shown in Figure 4. The measurements were taken in a small pressure chamber constructed of standard stainless steel pipe fittings, shown schematically in Figure 5. The measurements were performed with compressed helium under static conditions. The response has good linearity below 40 psia, but begins to saturate above that level. The non-linearity could be due to the diaphragm contacting the substrate, which is consistent with the P_{max} of a 0.8µm thick diaphragm shown in Table 1. However, the thickness of the diaphragm is non-uniform due to the nitride removal during the HF release etch.

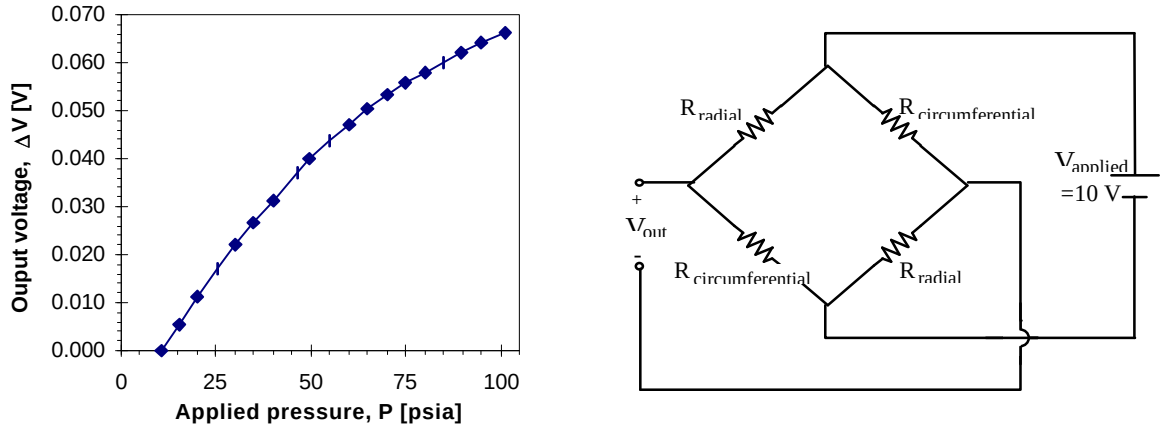

Figure 4. Output voltage and circuit schematic of pressure sensor.

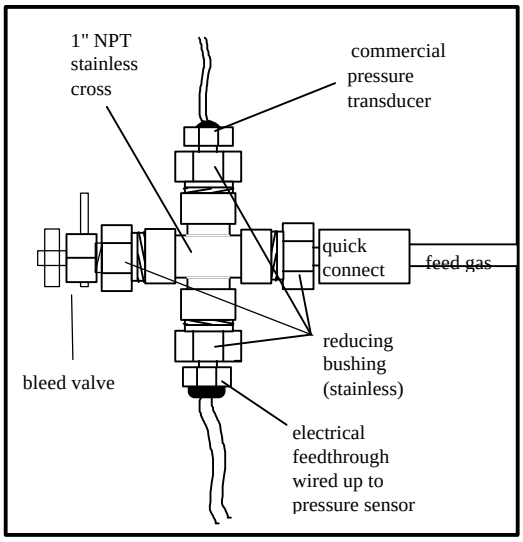

Figure 5. Pressure testing apparatus.

9. CONCLUSION

Surface micromachined piezoresistive pressure sensors were designed, fabricated, and tested at Sandia's Microelectronics Development Laboratory. These sensors were made from CMOS-compatible materials and were processed in the same tools as CMOS lots at the facility. These sensors measure absolute pressure by virtue of vacuum sealed diaphragms. By using an array of different sized diaphragms, a wide range of pressure sensitivities and frequency responses is achieved. Fabrication issues related to the release etch and metal step coverage were identified and addressed.

10. ACKNOWLEDGMENTS

Special thanks to Jeff Sniegowski, who provided design advice, and to the staff and operators of Sandia National Laboratories' Microelectronics Development Laboratory, without whom the devices could not have been made.

11. REFERENCES

[1] J.H. Smith, C.C. Barron, J.G. Fleming, S. Montague, J.C. Rodriguez, B.K. Smith, and J.J. Sniegowski, "Micro-machined sensors and actuators at the Microelectronics Development Laboratory," to be published in *Proceedings of Smart Structures and Materials '95*, SPIE, March 1995.

[2] L.A. Christel, M. Bernstein, R. Craddock, and K. Petersen, "Vibration rectification in silicon micromachined accelerometers", *Proceedings of the 7th International Conference on Solid-State Sensors and Actuators*, Transducers 93, IEEE Press, pp. 89-92 (1993).

[3] P.M. Morse, *Vibration and Sound*, Acoustical Society of America, pp. 208-214 (1981).

[4] D.W. Burns, "Micromechanics of integrated sensors and the planar processed pressure transducer," Ph.D. thesis, Department of Materials Science, University of Wisconsin - Madison, 1988.

[5] K.F. Dryden, "The Constant Current Loop: A New Paradigm for Resistance Signal Conditioning", *NASA Technical Memorandum* 104260 (1992).

[6] K.F. Anderson, *Sensors*, April 1994, pp.34-58.

[7] K.H.-L. Chau, C.D. Fung, P.R. Harris, and J.G. Panagou, "Over-range behavior of sealed-cavity polysilicon pressure sensors", *Sensors and Actuators A*, **28**, pp. 147-152 (1991).

[8] L. Lin, K.M. McNair, R.T. Howe, and A.P. Pisano, “Vacuum-encapsulated lateral microresonators”, *Proceedings of the 7th International Conference on Solid-State Sensors and Actuators*, Transducers 93, IEEE Press, pp. 270-273 (1993).

[9] P.J. French and A.G.R. Evans, “Piezoresistance in polysilicon and its applications to strain gauges”, *Solid-State Electronics*, 32 (1), pp. 1-10 (1989).

[10] L.H. Chang, “A study of PSG sacrificial etch solutions used in surface micromachining processing,” *Proceedings of the Symposium on Microstructures and Microfabricated Systems*, the Electrochemical Society, Vol 94-14, pp. 79-85.